

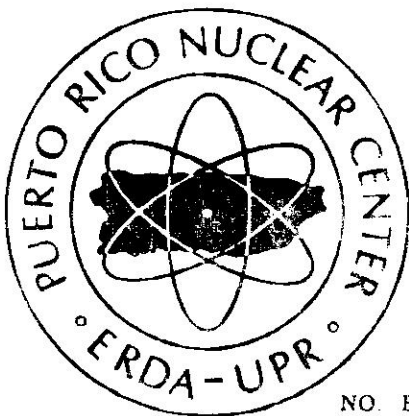
PRNC-205

PUERTO RICO NUCLEAR CENTER

ENVIRONMENTAL MONITORING
OF
ARGON - 41

By

Carlos Andreu and Donald S. Sasscer



OPERATED BY UNIVERSITY OF PUERTO RICO UNDER CONTRACT
NO. E-(40-1)-1833 FOR US ENERGY RESEARCH AND DEVELOPMENT ADMINISTRATION

ENVIRONMENTAL MONITORING

OF

ARGON - 41

by

Carlos Andreu *

and

Donald S. Sasscer

* Work performed at the Puerto Rico Nuclear Center in partial fulfillment of the requirements for the degree of Master of Science in Nuclear Engineering at the University of Puerto Rico at Mayaguez.

TABLE OF CONTENTS

TABLE OF CONTENTS	ii
LIST OF TABLES	iii
LIST OF FIGURES	iv
I INTRODUCTION	1
II REVIEW OF LITERATURE	4
III INSTRUMENTATION	5
IV METHOD AND RESULTS	9
V DISCUSSION OF RESULTS	36
VI CONCLUSIONS	42
REFERENCES	44
APPENDIX DECAY TIME	46

LIST OF TABLES

Table No.		Page
1.	Argon-41 Concentration Determination in the Off-Gas System	12
2.	Argon-41 Concentration Determination in the Surface of the Reactor Pool.	19
3.	Argon-41 Concentration Measured at the Stack	21
4.	Argon-41 Concentration Measured at Ground Level.	23
5.	Diffusion Coefficients	25
6.	Argon-41 Concentration Estimated at Ground Level	28
7.	Yearly Average Maximum Concentration and Dose Calculation	33

LIST OF FIGURES

Figure No.		Page
1.	Schematic Diagram of the High Sensitivity Counting System	8
2.	Overall Efficiency as a Function of Energy and the Four Inch Diameter by Four Inch High Cylindrical Na I Detector, 7.88 cm from the Source	11
3.	Kanne Chamber Calibration Curve	14
4.	Emission Rate of the Argon-41 in the Off-Gas System as a Function of Power Level	17
5.	Schematic Diagram of the Experimental Sample Collection Set Up	18
6.	Estimated and Measured Argon-41 Concentration at Ground Level	29
7.	Yearly Average Maximum Concentration at Ground Level for One-Shift Operation During the Dry and Rainy Season as a Function of Distance	30
8.	Yearly Average Maximum Concentration at Ground Level for Two-Shift Operation During the Dry and Rainy Season as a Function of Distance	31
9.	Maps of the Reactor Site Showing the Location of the Yearly Average Maximum Concentration	32

ABSTRACT

The objective of this work is to determine the yearly average maximum concentration and dose of argon-41 in unrestricted areas adjacent to the Puerto Rico Nuclear Center, and to develop a simple and accurate procedure for measuring argon-41 concentration, in order to verify the model used for calculation of the attenuation factor between the off-gas stack outlet and ground level. The model used is the diffusion equation for average long-period concentration from a continuous point source. In addition, the Kanne Chamber, which is the constant air monitor of the reactor off-gas system, was calibrated so as to enable an accurate and easy determination of the future concentration at any power level. The Kanne chamber was satisfactorily calibrated, with a probable error of approximately 5%.

The system used allows concentration at ground level to be measured to a factor of 6.75×10^5 less than the concentration emitted by the off-gas stack, or to approximately 1.6×10^{-10} $\mu\text{Ci/cc}$, which is 20% of the allowable concentration of 8.0×10^{-10} $\mu\text{Ci/cc}$. (1).

The average value of the ratio of the estimated to measured concentration is 1.1. This excellent agreement gives a high degree of confidence in utilizing the model to calculate the yearly average maximum concentration. The largest value of the yearly average maximum concentration occurred during one-shift operation, dry season, at 125 meters from the stack in the ENE sectors and is 2.69×10^{-10} Ci/meters^3 which is 33.6% of the allowable concentration.

The estimated dose corresponding to the largest yearly average maximum concentration is 0.53 mrem per year which is 5.3% of the allowable dose of 10 mrem per year. (1)

I INTRODUCTION

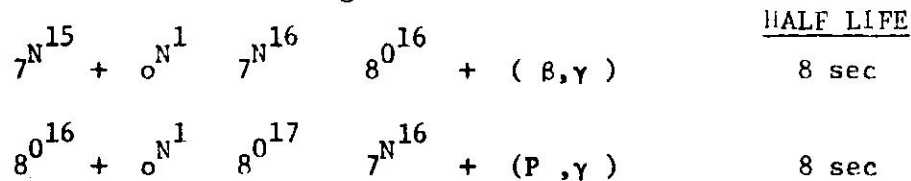
The sampling of air and the measurement of its radioactive content is often a difficult task due to variable sampling conditions, the diversity of the radioactive substances being sampled, and the fact that there are no standardized air sampling instruments or equipment that can be used for all situations.

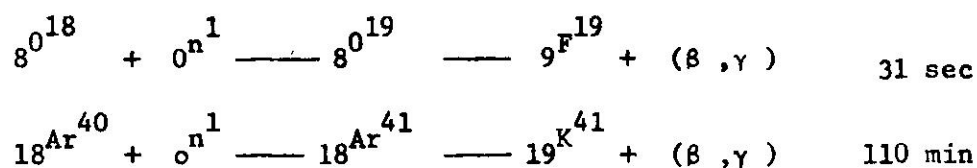
The natural environment has always contained a certain amount of radioactivity. With the discovery and application of radioactive substances and the increasing use of research and power reactors, another potential environmental contaminant has been created, thus necessitating a closer scrutiny of various environmental media, including air.

Discharges of radioactive waste to the environment by the Puerto Rican Nuclear Center (PRNC) are regulated by the Energy Research and Development Administration.

The PRNC, functioning as a training and research center, is engaged in a wide variety of activities some of which involve the TRIGA-FLIP reactor. Such operations invariably produce quantities of gaseous wastes known to contain radioactive nitrogen, oxygen and argon. They are formed from the neutron bombardment of the air contained in the thermal column, beam tubes, gamma room, in-core and side core rabbit system and from the water in the reactor pool.

The formation occurs according to





The half lives of the isotopes of nitrogen and oxygen which become radioactive are so short that they decay before escaping from the reactor building. Substantially all of the activity in the air or water under normal operating conditions is due to argon-41.

During normal operation, pool water circulates through the reactor by natural convection, thereby exposing the air which is dissolved in the water to the neutron flux of the core. At the same time that the argon in this air is activated, a fraction of it is driven off from the water due to the reduced air solubility as the water temperature increases in its passage through the core. Once the air is driven off, part of it re-dissolves as it bubbles up through the water and part of it reaches the pool surface and mixes with the building air. It is then exhausted through the normal 16000cfm ventilation system, 69 feet above the site boundary.

In addition, air is circulated through the thermal column volume and the dry beam tubes and the two rabbit systems by the off-gas system blower. Of the six beam-tube positions, three contain neutron spectrometer collimators and are not connected to the off-gas system. A fourth one is out of commission and removed from the reactor. Of the remaining two, one is operated in the flooded condition so that only one beam tube is being swept by the off-gas system. The argon in this air and the air of the rabbit system is therefore activated and drawn off to the atmosphere by the off-gas blower. This is a 150cfm blower exhausting to the atmosphere at a level of 50 feet above the site boundary fence.

Since radioactive argon is the main source of gaseous activity produced by the PRNC TRIGA reactor during normal operation, the primary objective of this work was to develop a simple and accurate procedure for measuring argon-41 concentration at ground level, in order to verify diffusion equation for average long-period concentration from a continuous source. This model was used for calculating the attenuation factor between the off-gas stack outlet and ground level. In addition, the Kanne chamber, which is the air monitor of the reactor off-gas system was calibrated so as to enable an accurate and easy determination of the concentration in the future at any power level.

II REVIEW OF LITERATURE

Research has been performed on this problem by Efigenio Rivera from Health Physics Division in 1973 (2). This work included the determination of the concentration of argon-41 bubbles emerging from the pool surface and all of the argon-41 through the off-gas system. Also, the Kanne chamber was calibrated utilizing the argon-41 produced in the reactor core and emerging through the pool water as the calibrated source.

In addition, Pedro Cruz from the Puerto Rico Nuclear Center Reactor Division (3) includes the calibration of the Kanne chamber, using krypton-85 as the standard. The experiment was conducted statically by feeding a known concentration of krypton-85 into the chamber. For each concentration the meter readings in μA amp recorded and plotted as a function of the known concentration in $\mu\text{Ci/cc}$.

Other research related to the Kanne chamber refer to the efficiency determination of a Kanne chamber for detection of radiogases by J. J. Fitzgerald and B. W. Borelli (4). The inventor of the Kanne chamber, W. R. Kanne, reported a device for the monitoring of gas for radioactivity (5) and for the monitoring of gas for radioactive xenon (6). These works describe in detail the Kanne chamber and its principle of operation.

The literature survey revealed the existence of other works done in similar areas but not directly related or applicable to this research.

III INSTRUMENTATION

A. FOR THE EFFICIENCY DETERMINATION OF THE DETECTION SYSTEM

A four inch diameter by four inch height cylindrical sodium iodide crystal activated with thallium was used for the detection of gamma rays. The detector was connected to a preamplifier and linear amplifier. Pulse height analysis was done by a multichannel analyzer (Series 2200 Nuclear Data Analyzer) with the end result typed or displayed on an oscilloscope. A high voltage power supply was utilized to provide a regulated voltage to the photomultiplier tube.

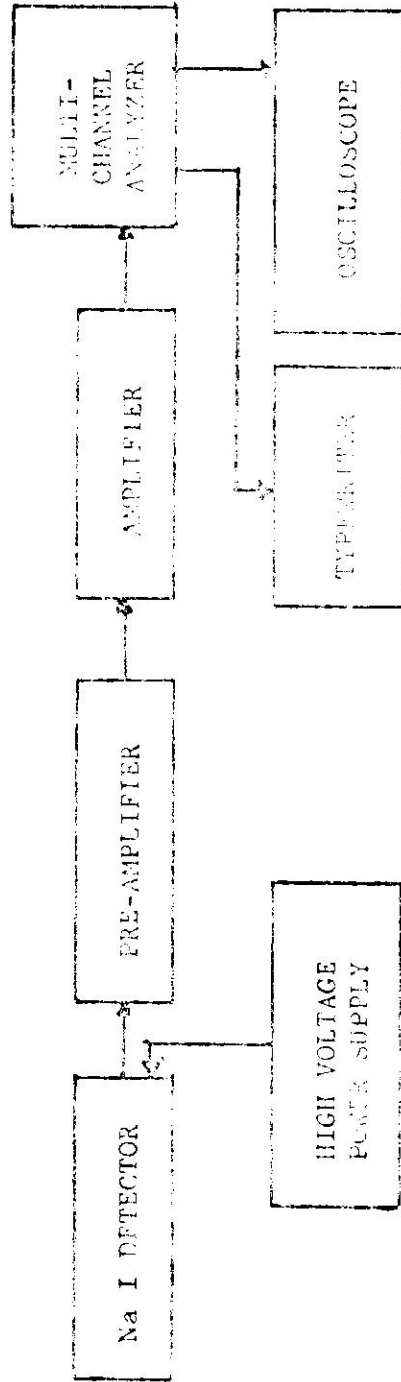
B. FOR THE DETERMINATION OF THE ARGON-41 CONCENTRATION

1. In the off-gas system
2. At the surface of the reactor pool

The instrumentation described in "A" immediately above, was used to determine the argon-41 concentration in both the off-gas system and above the reactor pool.

3. At various ground level locations

The measurements of the argon-41 concentrations at various ground level locations required a high-sensitivity counting system. This high-sensitivity counting system was developed by: a) increasing the shielding to six inches of lead, b) connecting two sodium iodide detectors in parallel, and c) obtaining samples of air by using a high pressure pump to fill a scuba tank to a pressure of 2200 psi. The rate of air entering the tank was found to be constant with time. (See Figure 1).



Block Diagram of the Gamma Counting Equipment

Of the two detectors used, one was the four inch by four inch detector described above, and the one was a three inch by three inch sodium iodide crystal. Each was connected to a high voltage supply, a preamplifier and a linear amplifier. These two connections were introduced to the multichannel analyzer (Series 2200 Nuclear Data Analyzer) for the pulse height analysis. The results were shown in an oscilloscope and typed.

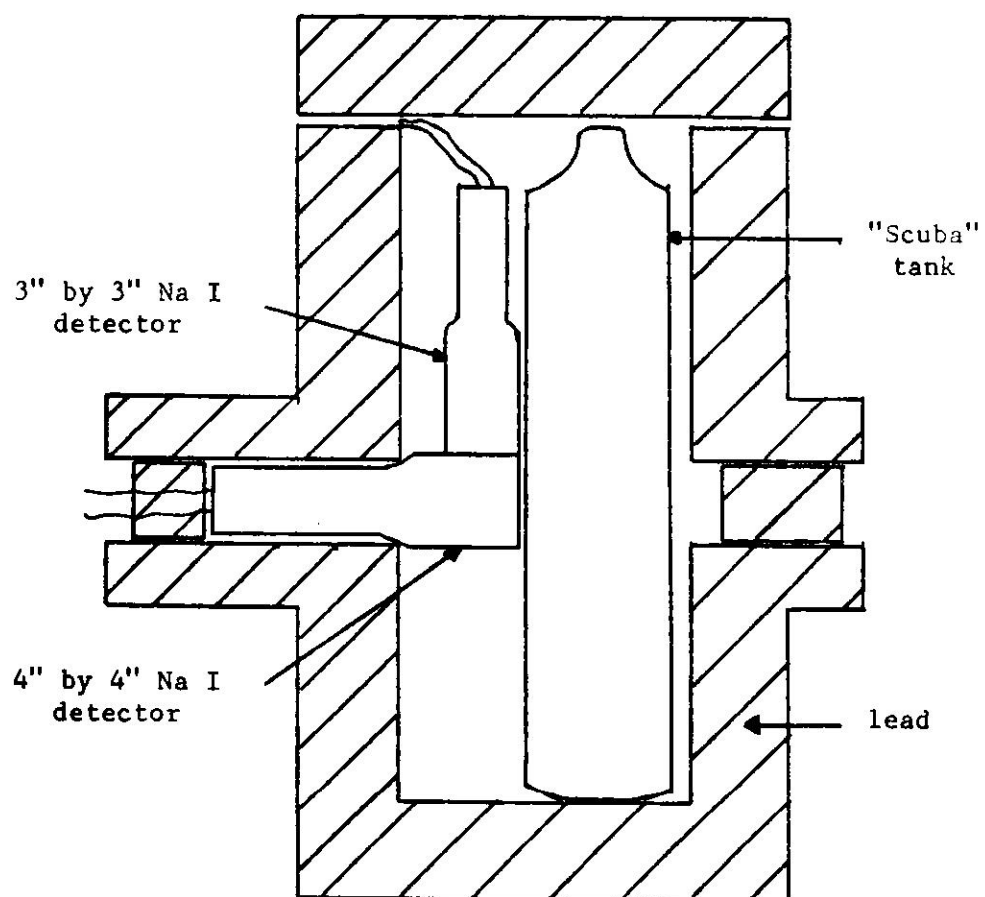


Fig. 1. Schematic Diagram of the High-Sensitivity Counting System

IV METHOD AND RESULTS

A. OVERALL EFFICIENCY DETERMINATION OF THE DETECTION SYSTEM FOR THE 1.29 Mev GAMMA OF ARGON-41

An efficiency calibration curve was made for the detection system of argon-41. A sodium-22 source (which emits a gamma of 1.27 Mev 100% of the time) and a cesium-137 source (which emits a gamma of 0.662 Mev 93.5% of the time) were used as standard sources for the determination of the efficiency. Each source was placed at the same distance from the detector (7.88 cm) and the overall peak efficiency for the count system at each energy was found using Equation 1.

$$\text{EFFICIENCY (\%)} = \frac{\text{AREA}}{(\text{ACTIVITY}) (\text{PROBABILITY})} \times 100$$

PROBABILITY = Probability of emitting a gamma of that energy per disintegration

ACTIVITY = Present activity of source (disintegration/sec)

AREA = Response of system to the source determined using the Total Peak Area Method (counts/sec)

where:

$$\text{AREA} = \sum_{i=L}^{i=R} A_i - A_L + A_R) \frac{(R - L + 1)}{2}$$

A_i = Number of counts accumulated in channel i

L = Channel number at left hand limit of photopeak

R = Channel number at right hand limit of photopeak

The overall efficiency for the 1.27 Mev peak of Na-22 and the 0.662 Mev peak of Cs-137 was determined to be 1,317% and 2.29% respectively, for the detection system described in section III-A.

Using the efficiency calibration curve of Figure 3, the overall efficiency of the 1.29 Mev peak of argon-41 was determined to be 1.3%.

An efficiency curve obtained from reference (7) for a typical four inch by four inch sodium iodide detector is also shown in Figure 2.

B. DETERMINATION OF THE ARGON-41 CONCENTRATION

1. In the off-gas system

Argon-41 concentration in the off-gas system was determined by taking samples in a 1000 cc spherical glass container with a stopclock valve. The container was previously evacuated to a pressure of approximately 0.1 mm of mercury for each sample. Each time a sample was collected, the time of collection, start counting time, power level of the reactor, air flow through the stack and Kanne chamber readings were recorded. (See Table 1).

In order to apply the counting efficiency of the system as obtained from point sources in Section IV-A to a much larger volume, a geometry factor is needed. Since this factor had already been obtained by Efigenio Rivera in his thesis (2) and the same container and geometry as used by Rivera was used in this work (7.88 cm as the distance from the exact center of the 1000 cc sphere to the detector), it was possible to use his geometry factor for correcting the point source assumption. This correction factor is 0.950 for 1000 cc sphere.

Counts of 10000 second, live time, were obtained for each sample.

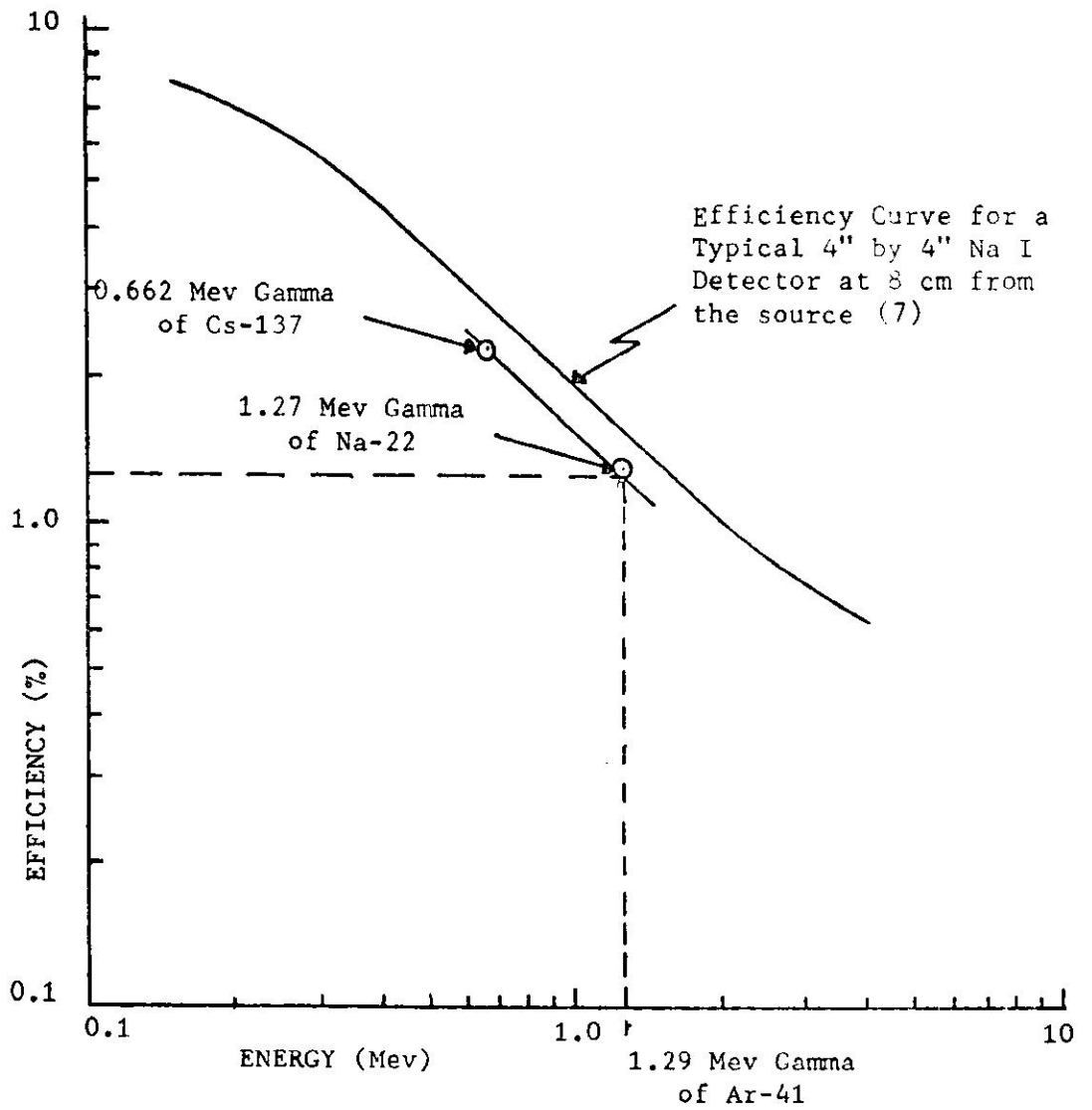


Figure 2. Overall Efficiency as a Function of Energy of the Four Inch Diameter by Four Inch High Cylindrical Na I Detector, 7.88 cm from the Source.

Table 1. Argon-41 Concentration Determination in the Off-Gas System

* Power Level (Kw)	* Kanned Chamber Readings (amp)	T.P.A.* ($\frac{\text{disintegration}}{\text{sec-cc}}$)	Decay** Time (sec)	Concentration ($\mu\text{Ci/cc}$)	Air Flow* (cc/min)	Emission Rate ($\mu\text{Ci/min}$)
250	1.12×10^{-11}	0.0068898	4746	2.53×10^{-5}	5179728	130.8
500	2.25×10^{-11}	0.0144613	4746	5.30×10^{-5}	5080608	269.3
750	3.50×10^{-11}	0.0218106	4686	7.99×10^{-5}	5066448	405.0
1000	4.80×10^{-11}	0.0304929	4746	11.18×10^{-5}	5137248	569.7
1000	4.80×10^{-11}	0.0283649	4746	10.40×10^{-5}	5089104	529.1
1000	4.50×10^{-11}	0.0289596	4866	10.61×10^{-5}	4975824	528.1
1000	4.70×10^{-11}	0.0309736	4686	11.35×10^{-5}	4933344	560.0
1000	4.50×10^{-11}	0.0289487	4746	10.61×10^{-5}	5063616	537.2
1000	4.60×10^{-11}	0.0291415	4746	10.68×10^{-5}	5001312	534.2

* Data Recorded

In order to keep the same overall efficiency as was determined in Section IV-A, the 1.29 Mev argon-41 peak was determined in the same way as the 1.27 Mev sodium-22 peak. Total Peak Area Method (explained in Section IV-A) was used to calculate the area under the peak. Since this area is not representative of the activity in the off-gas system at the instant of collection, it had to be corrected for decay time. (See Appendix).

Therefore, the argon-41 concentration in the off-gas system at the instant of collection is given by

$$A_0 = \frac{(T.P.A.)(e^{\lambda T})}{E_f (V.C.F.)(3.7 \times 10^4)} \quad (\mu\text{Ci/cc}) \quad (2)$$

where

T.P.A.	is the total peak area in counts/sec per cc
$e^{\lambda T}$	is the time decay correction factor
E_f	is the efficiency of the counting system
3.7×10^4	is the conversion factor from disintegration/sec to μCi
V.C.F.	is the volume correction factor for the 1000 cc collection sphere

Results are presented on Table 1.

a. Kanne chamber calibration

Radioactive argon-41 concentration in the off gas system is continuously monitored by a Kanne chamber. The Kanne chamber was accurately calibrated in order to have confidence in future readings. The calibration was performed using the data obtained from the off-gas system concentration determination. (See Table 1). A line to correlate the recorded Kanne chamber reading and the determined argon-41 concentration was drawn by linear regression analysis. (See Figure 3.).

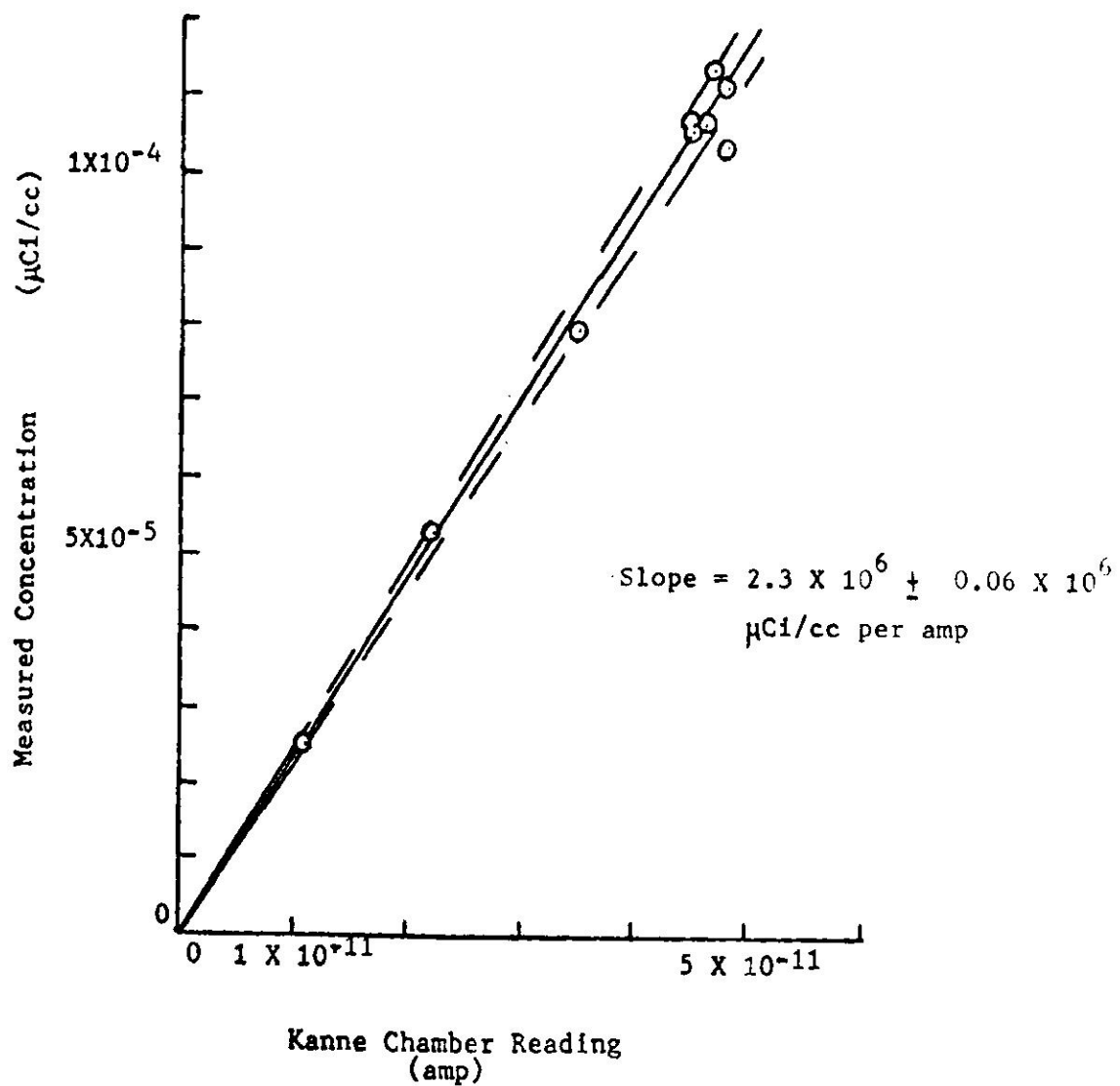


Figure 3 . Kanne Chamber Calibration Curve

These data gave a conversion factor between Kanne chamber reading and concentration in $\mu\text{Ci/cc}$ of

$$\text{Concentration } (\mu\text{Ci/cc}) = (2.3 \times 10^6 + 0.06 \times 10^6) \times (\text{Kanne chamber reading}) \quad (3)$$

This indicated that the probable error in the conversion of Kanne chamber to a concentration is approximately 5%.

b. Emission rate variation with power level

The argon-41 emission rate should be proportional to the flux or power level. Since the samples were taken at different power levels, (See Table 1) a line was drawn to check the linearity of the activity of argon-41 production as a function of power (See Figure 4). This line gave an average emission rate of $543 \mu\text{Ci/min}$ with a probable error of 6% at 1000 Kw.

2. At the surface of the reactor pool

Since the area where the argon-41 emerged through the reactor pool water was large, a sheet metal cone was placed on top of the water surface to collect some of the effluent gas. A polyethylene tube was connected to the collector, and to one side of a three-way glass valve. One valve outlet provided means for sample drawing at any time, the other outlet was connected to another section of the tube with its end under two inches of water. (See Figure 5). This was done in order to determine the volume rate in cc/min of argon-41 effluents. The area occupied by the collector on top of the pool surface was approximately one half of the total area through which the argon-41 effluent was emerging. Therefore, since

the volume rate collected was measured to be 133 cc/min, the total argon-41 effluent released into the reactor building was estimated to be 300 cc/min.

Using Equation 2 the concentration of argon-41 at the pool surface was obtained and is presented in Table 2.

3. At various ground level locations

a. Sensitivity of counting system

The high sensitivity of the new counting system (discussed in Section III-B-3), without taking into consideration the increased pressure, was determined before the system was used. This was done by taking a sample of the off-gas in a scuba tank (previously evacuated to a pressure of 0.4 mm of mercury) at the stack. The tank was filled to atmospheric pressure. Activity for periods of 4000 seconds were obtained for almost 24 hours. In all of the sixteen runs the argon-41 peak was present even though the last run was counted 12.5 half lives after the sample had been taken. This could be done because the background was reduced and the efficiency was increased by a factor of two.

A curve of the activity as a function of time was obtained and the decay constant was found as $1.042 \times 10^{-4} \text{ sec}^{-1}$ which is very near to the accepted value of $1.052 \times 10^{-4} \text{ sec}^{-1}$.

The method explained above gave the sensitivity of the counting system taking into consideration only the increase in shielding and in the efficiency. This gave an initial to final count ratio of approximately 4500, when the air in the tank was at atmospheric pressure.

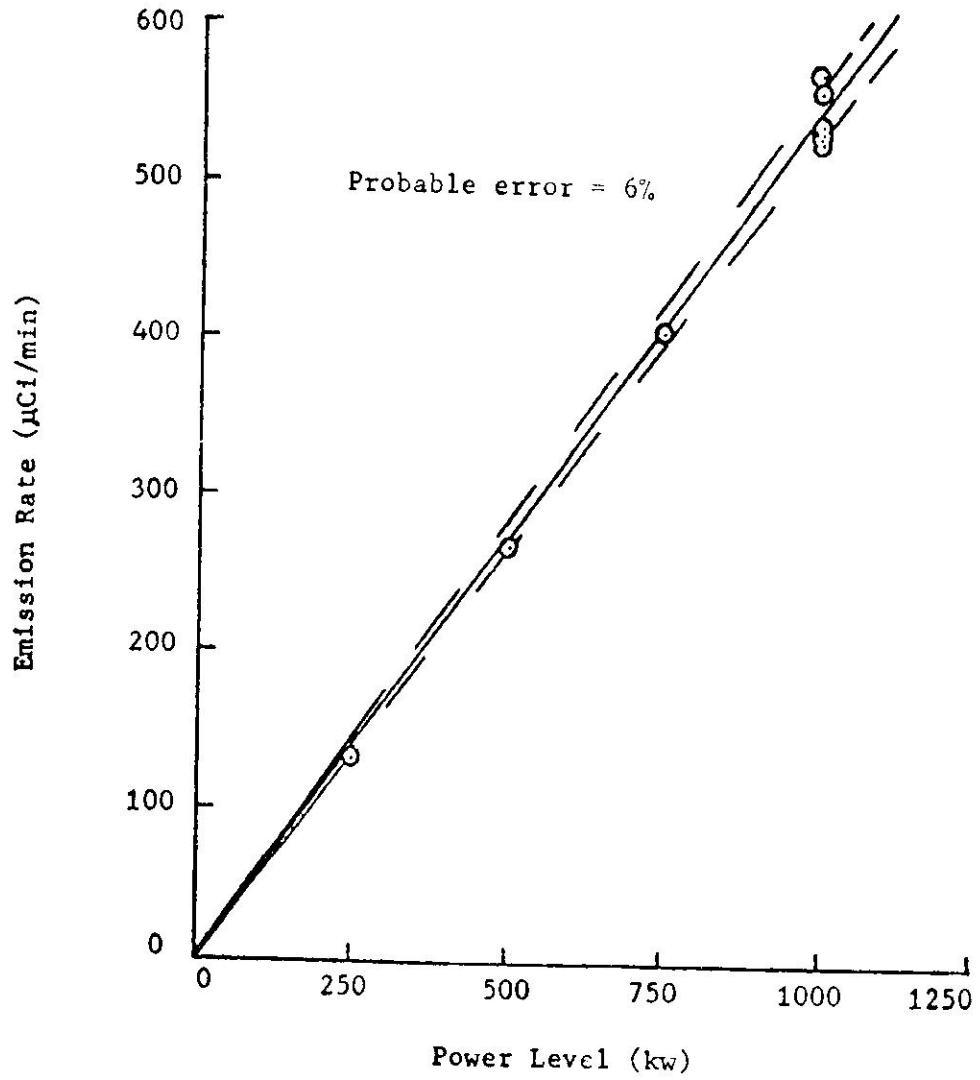


Figure 4. Emission Rate of Argon-41 in the Off-Gas System as a Function of Power Level.

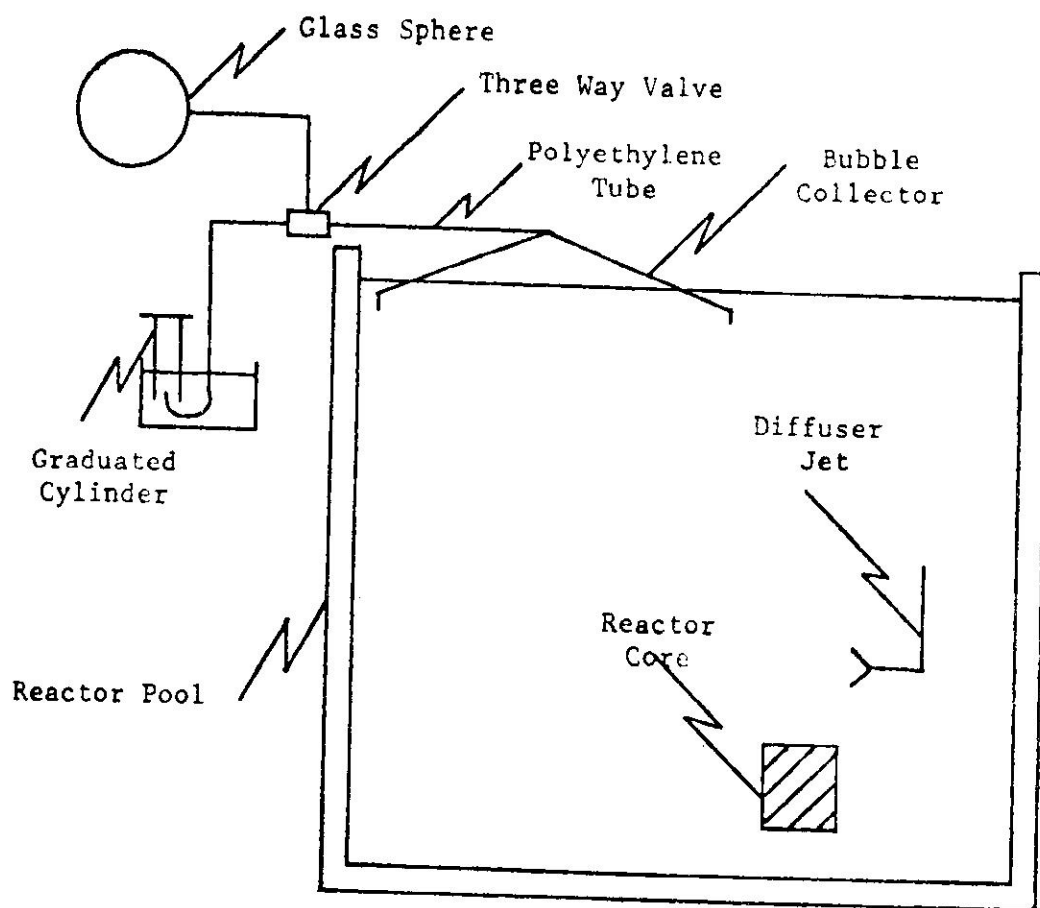


Figure 5. Schematic Diagram of the Experimental Sample Collection Set Up.

Table 2. Argon-41 Concentration Determination
in the Surface of the Reactor Pool

Power* Level (Kw)	T.P.A.* ($\frac{\text{desintegration}}{\text{sec-cc}}$)	Decay* Time (sec)	Concentration ($\mu\text{Ci/cc}$)	Air Flow* (cc/min)	Emission Rate ($\mu\text{Ci/min}$)
1000	0.751999	12027	6.38×10^{-3}	300	1.698
1000	310207	650	6.98×10^{-3}	300	1.852

*Data Recorded

However, the sensitivity was increased by a factor of 150 by collecting air in a scuba tank at a pressure of 2200 psi. Therefore, the system can determine concentrations to approximately 150 times 4500 or 6.75×10^5 times less than the concentration leaving the off-gas stack. The concentration in the off-gas system is approximately 10.8×10^{-5} $\mu\text{Ci/cc}$ at the 1000 Kw power level. Therefore, the system can determine concentrations to approximately 1.6×10^{-10} $\mu\text{Ci/cc}$, which is less than 20% of the allowable concentration of 8×10^{-10} $\mu\text{Ci/cc}$ (1).

b. Measured value

Using the high sensitivity system described above, samples of air at various ground level locations were obtained in a scuba tank which was filled to a pressure of 2200 pounds per square inch. This pressure was obtained using a scuba tank air compressor. Each tank was previously evacuated to a pressure of 0.4 mm of mercury. Counts of 4000 seconds (live time) were taken for each sample. For every sample the following was recorded: Kanne chamber reading, air flow coming out of the stack, distance from the stack to the sampling location, wind speed, wind direction, wind frequency to the sampling location, meteorological conditions, time at start of collection, start counting time, and pressure of the tank after finishing the countings. All of these parameters were needed. Some to calculate the measured values, others for the estimated values.

Using the Kanne chamber reading, the argon-41 concentration at the stack could be determined from the calibration curve. Using Equation 3.

$$\text{Concentration at the stack} = (\text{Kanne chamber})(\text{Conversion factor})$$

Table 3. Argon-41 Concentration Measured at the Stack

Corresponding to Table 5 Run No.	Date*	Sample* Taken	Decay* Time (sec)	Activity* ($\frac{\text{Counts}}{4\text{Ksec-tank}}$)	Activity Corrected for Decay ($\frac{\text{Counts}}{4\text{Ksec-tank}}$)	Kanne* Chamber Readings (amp)	Concentration at the Stack ($\mu\text{Ci/cc}$)	Air Flow*Emission Rate (cc/min) ($\mu\text{Ci/min}$)
1, 2, 3, 4, 5	2/27/75	3:21 P.M.	217960	203107	364543	4.5×10^{-11}	10.3×10^{-5}	4216848 435.2
6	2/20/75	3:23 P.M.	2110	481813	579239	5.1×10^{-11}	11.1×10^{-5}	4534032 530.6

*Data Recorded

or

$$10.3 \times 10^{-5} = (4.5 \times 10^{-11})(2.30 \times 10^6).$$

If the tank is filled with argon-41 to atmospheric pressure at the stack, and counted with the same geometry and efficiency as the one filled at ground level, we can determine the argon-41 concentration at ground level using the following relation.

$$\frac{\text{Concentration at ground level}}{\text{Concentration at the stack}} = \frac{\text{Activity at ground level}}{\text{Activity at stack}} \quad (5)$$

where appropriate corrections are made for counting and decay time.
(See Appendix)

The activity at ground level (Table 4) and the activity at the stack (Table 3), to which the ground measurements were compared, were obtained the same day in order to minimize the error determining the attenuation factor between the stack and ground level.

c. Calculated value

Three meteorological factors are of significance in determining the amount of mixing which will occur to contaminants in the event of diffusion into the atmosphere. They are: the distribution of temperature with height, the surface wind direction and speed and the precipitation.

A complete mathematical analysis of diffusion processes which would allow quantitative calculations of concentration is difficult because instantaneous velocities exhibit irregular and random fluctuations. Equations currently in use are based in part on statistical analysis and must necessarily include some constants which are empirical in nature. These constants are functions of eddy diffusion and parameters which

Table 4. Argon-41 Concentration Measured at Ground Level

Run Number	Distance from the Source* (Meters)	Date*	Start Pump Time*	End Pump Time*	Start Count Time*	Decay Time* (sec)	Activity* $\left(\frac{\text{Counts}}{4\text{Ksec-tank}}\right)$	Activity Corrected for Decay $\left(\frac{\text{Counts}}{4\text{Ksec-tank}}\right)$	Pressure in Tank after Counts* (Atmospheres)	Measured Concentrations at Ground Level (pCi/cc)
1	117	2/27/75	7:53 A.M.	8:24 A.M.	8:31 A.M.	3280	-1	—	138.8	—
2	117	2/27/75	10:12 A.M.	10:43 A.M.	10:49 A.M.	3220	29	41	139.5	8.32×10^{-11}
3	117	2/27/75	11:37 A.M.	12:08 P.M.	12:23 P.M.	3760	606	900	148.3	1.72×10^{-9}
4	117	2/27/75	1:02 P.M.	1:34 P.M.	1:46 P.M.	3610	717	1048	148.7	2.00×10^{-9}
5	117	2/27/75	2:29 P.M.	3:01 P.M.	3:09 P.M.	3370	268	382	146.3	7.39×10^{-10}
6	90	2/21/75	3:01 P.M.	3:32 P.M.	3:36 P.M.	3100	1568	2173	139.5	3.15×10^{-9}

*Data Recorded

depend on atmospheric stability. Determining suitable values for these coefficients and parameters is the most important operation in their application. Suggested diffusion coefficients for the PRNC, Mayaguez, are shown in Table 5 and are obtained from Reference 8.

The concentration of argon-41 as a function of distance from a continuous, long term, point release of gas was calculated from Equation 3.143 or Reference 9 for the cross wind integrated concentration.

$$\bar{X}_{cwi} = \frac{2}{\pi} \frac{1}{2} \frac{Q'}{\sigma_z \mu} \frac{-h^2}{2\sigma_z^2} \quad (6)$$

where the standard deviation of the distribution of material in a plume in the Z direction, σ_z is determined by the Sutton form (Sec 8-4) of (9) to be

$$\sigma_z^2 = 1/2 C_z^2 X^{(2-n)}$$

If the concentration is averaged over a 22.5 section (1/16 of a circle), then the long-term average concentration is given by

$$\bar{X} = \frac{2}{\pi} \frac{0.01 f Q'}{\sigma_z \mu \frac{2\pi}{N}} \exp \frac{-h^2}{2\sigma_z^2} \quad (7)$$

where

C_z = diffusion coefficient in the z-plane (meters)^{n/2}

X = distance from the source (meters)

n = nondimensional parameter associated with stability

f = percent of frequency with which the wind blows from a given sector

Q' = rate of material emission from a continuous point source (Ci/sec)

μ = mean wind speed (meter/sec)

h = height of source (meter)

$\frac{2\pi X}{N}$ = is the sector width for each of N sectors at the distance X (N = 16)

\bar{X} = concentration of argon-41 (Ci/meter²)

Table 5. Diffusion Coefficients

	n	C _y	C _z
Weak Lapse Rate (Adiabatic)	0.25	0.26	0.14
Isothermal or Slight Inversion	0.30	0.20	0.10
Large Inversion, Stable Conditions	0.50	0.13	0.05

Table 6 presents the estimated argon-41 concentration at ground level and Figure 6 shows the relationship between the estimated and measured argon-41 concentrations.

d. Yearly average maximum concentration

To determine the yearly average maximum concentration of argon-41, the average velocity and frequency of wind in each 22.5° directional sector was obtained on an hourly basis for the dry and wet season from the climatology data of PRNC-37, Section IV, Appendix A, (8). The hourly values were averaged between 8:00 a.m. and 3:00 p.m. to obtain the average wind velocity and frequency per sector for one-shift operation. For the two-shift operation, the hourly values were averaged between 8:00 a.m. and 6:00 p.m. (11 hours of day), and 7:00 p.m. and 11:00 p.m. (5 hours of night). The division between night and day was necessary due to the fact that in Mayaguez the nights have 90% probability of large temperature inversion and the days a high probability of adiabatic conditions (8). Therefore, to determine the concentration, two sets of diffusion constants had to be used, one for the day and one for the night. (See Table 5).

For the dry season, during both one-shift and two-shift operations, the concentration was greatest in the ENE sector. In the rainy season the greatest value of concentration for both operations was in the W sector. Although the SW sector and the ENE sector have almost the same frequency-to-velocity factor during the dry season, and W and SSW sectors have also almost the same frequency-to-velocity factor during the rainy season, the ENE and the W sectors had the highest concentration due to the elevation of land in these sectors, giving a smaller effective stack height.

The emission rate for the 1000 Kw power level was assumed to be $9.0 (10^{-6})$ Ci/sec based on the emission rate as a function of power level of Figure 4.

Substituting the values of Table 7 for each separate condition in Equation 7, the concentrations as function of distance were determined and are presented in Figure 7 and 8. The distance from the source, at which the yearly average maximum concentration occurs, was determined from these figures.

The 1000 Kw power level yearly average maximum concentration of argon-41 in uncontrolled areas, during one-shift and two-shift operations, during the dry and the wet seasons, is shown in Table 7.

The locations of the maximum concentration are shown in Figure 9.

C. YEARLY AVERAGE MAXIMUM DOSE CALCULATIONS

1. Internal dose

The cumulative dose, from the beginning of exposure, due to a finite inhalation time was calculated using Equation 7.101 of Reference 9.

$$D_{co} = \frac{5.92 (10^2)}{M \lambda^2} E f_a B' \bar{X} (\lambda t - e^{-\lambda t} + e^{-\lambda(t+t')}) \quad (8)$$

where

\bar{E} = energy absorbed in the organ from one disintegration (Mev)

M = mass of the organ (gm)

f_a = fraction of radionuclide transferred to the organ retention factor

B' = breathing rate (meters³/sec)

\bar{X} = yearly average maximum concentration (Ci/meters³)

$$\lambda = (\lambda_R + \lambda_B) = \left(\frac{0.693}{T_R} + \frac{0.693}{T_B} \right)$$

Table 6. Argon-41 Concentration Estimated at Ground Level

Run Number	Distance from the Source* X (Meters)	Wind Frequency* f (%)	Wind Speed* \bar{u} (Meters/sec)	Meteorological Conditions*	Height of Source* h (Meters)	Kann Chamber Readings* (amp)	Concentration at the Stack ($\mu\text{Ci/cc}$)	Air Flow Rate* (cc/sec)	Emission Rate Q' (Ci/sec)	Estimated Concentration at Ground Level X ($\mu\text{Ci/cc}$)
1	117	—	1.47	Adiabatic	10	—	—	—	—	—
2	117	33	1.88	Adiabatic	10	4.4×10^{-11}	9.98×10^{-5}	71319	7.12×10^{-6}	9.99×10^{-10}
3	117	100	3.52	Adiabatic	10	4.5×10^{-11}	10.32×10^{-5}	70564	7.28×10^{-6}	1.65×10^{-9}
4	117	100	2.20	Adiabatic	10	4.5×10^{-11}	10.32×10^{-5}	70753	7.30×10^{-6}	2.64×10^{-9}
5	117	98	4.92	Adiabatic	10	4.5×10^{-11}	10.32×10^{-5}	70281	7.25×10^{-6}	1.17×10^{-9}
6	90	100	3.35	Adiabatic	10	4.8×10^{-11}	11.01×10^{-5}	84960	9.35×10^{-6}	1.78×10^{-9}

*Data Recorded

Assumption of adiabatic conditions based on private communication with International Airport Weather Station, Isla Verde, Puerto Rico.

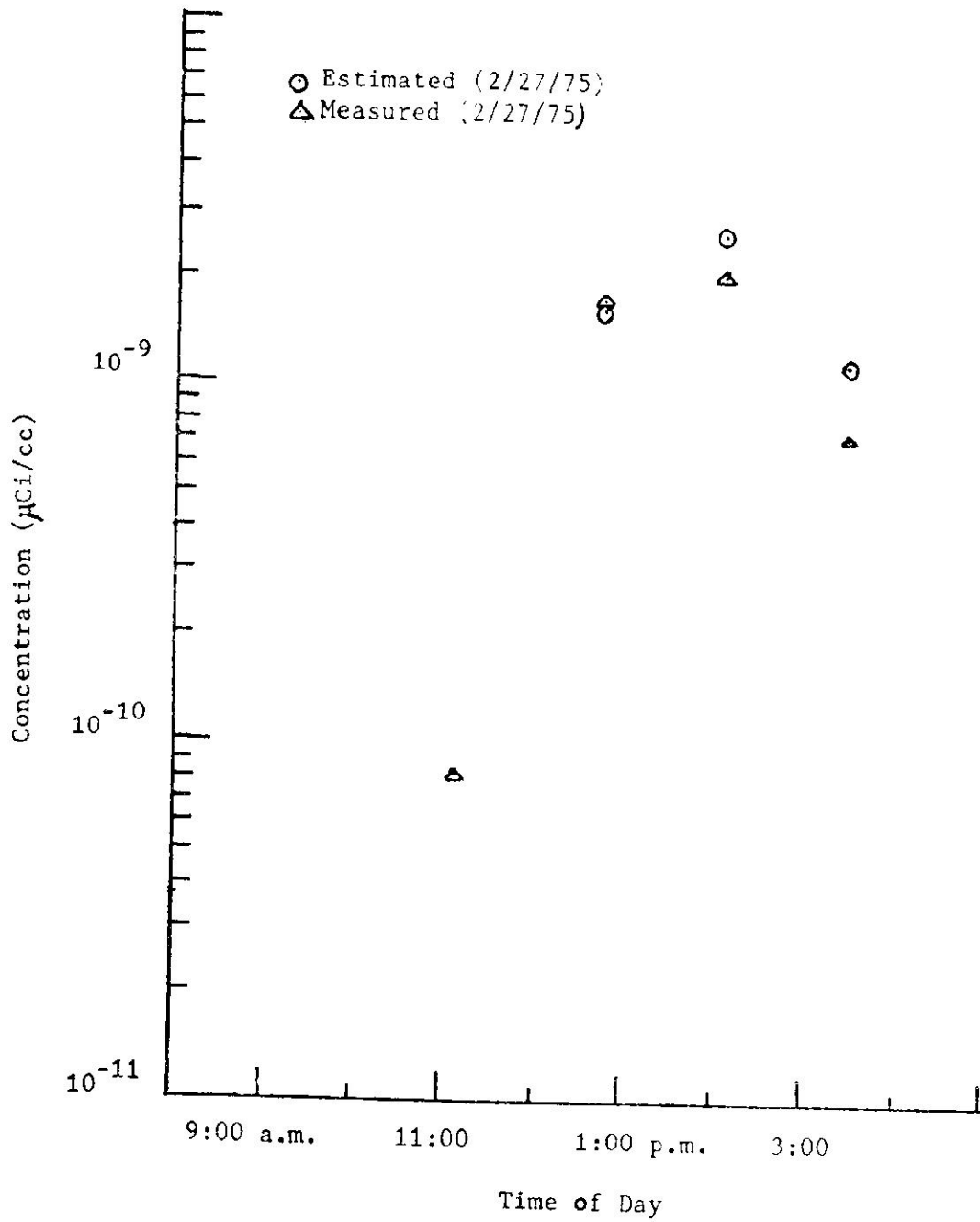


Figure 6. Estimated and Measured Argon-41 Concentration at Ground Level.

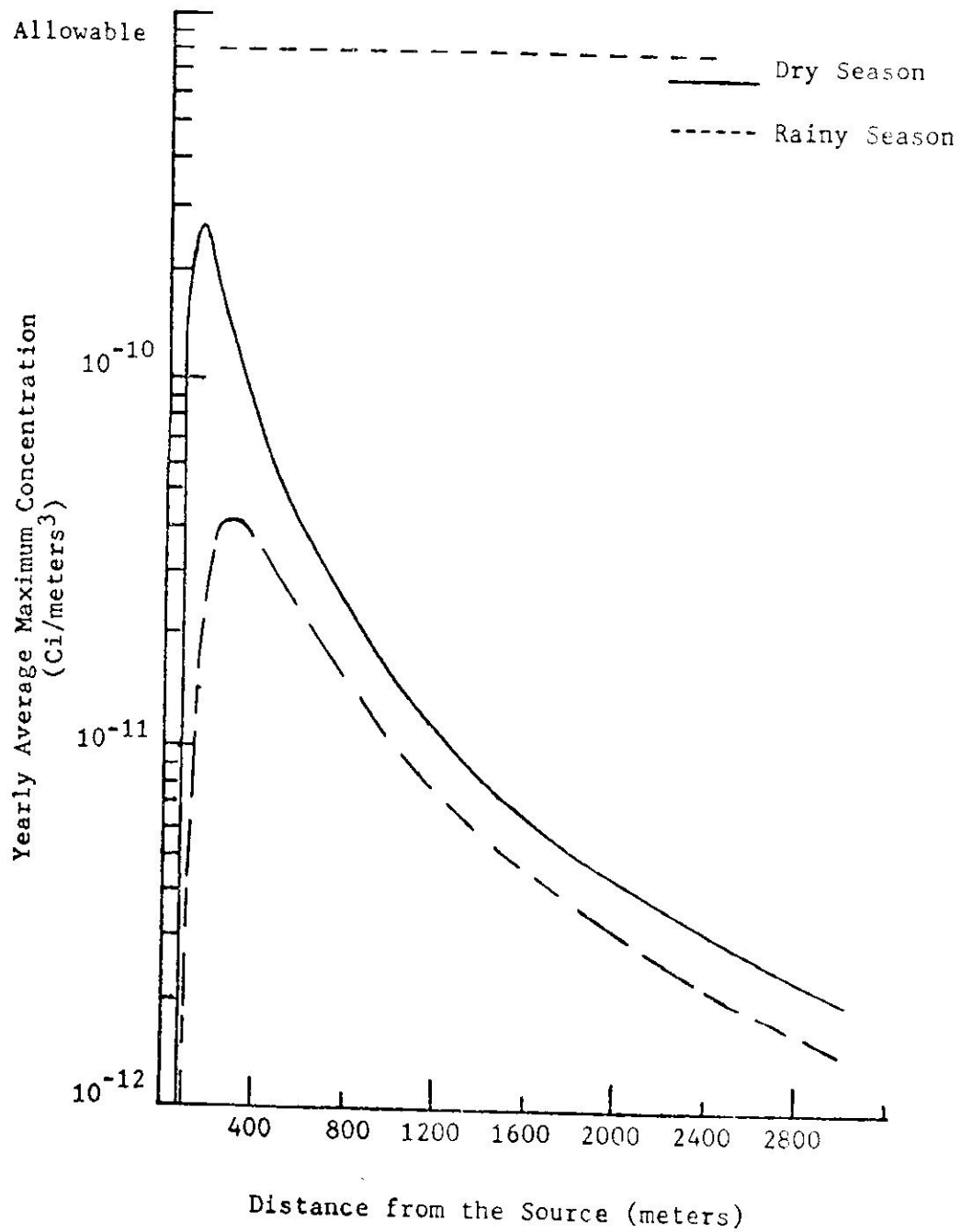


Figure 7. Yearly Average Maximum Concentration at Ground Level for One-Shift Operation During the Dry and Rainy Seasons as a function of Distance.

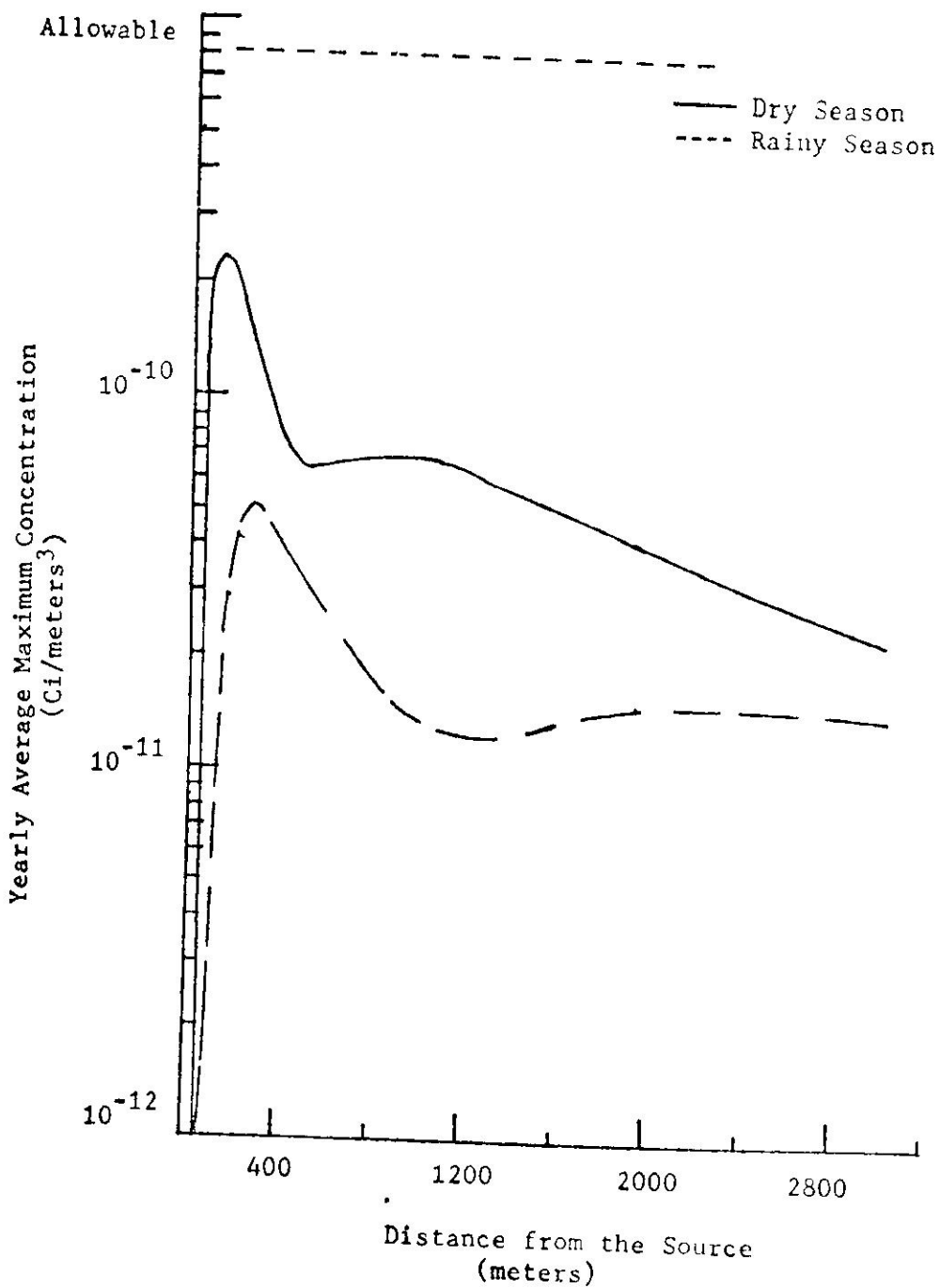


Figure 8. Yearly Average Maximum Concentration at Ground Level for Two-Shift Operation During the Dry and Rainy Seasons as a Function of Distance.

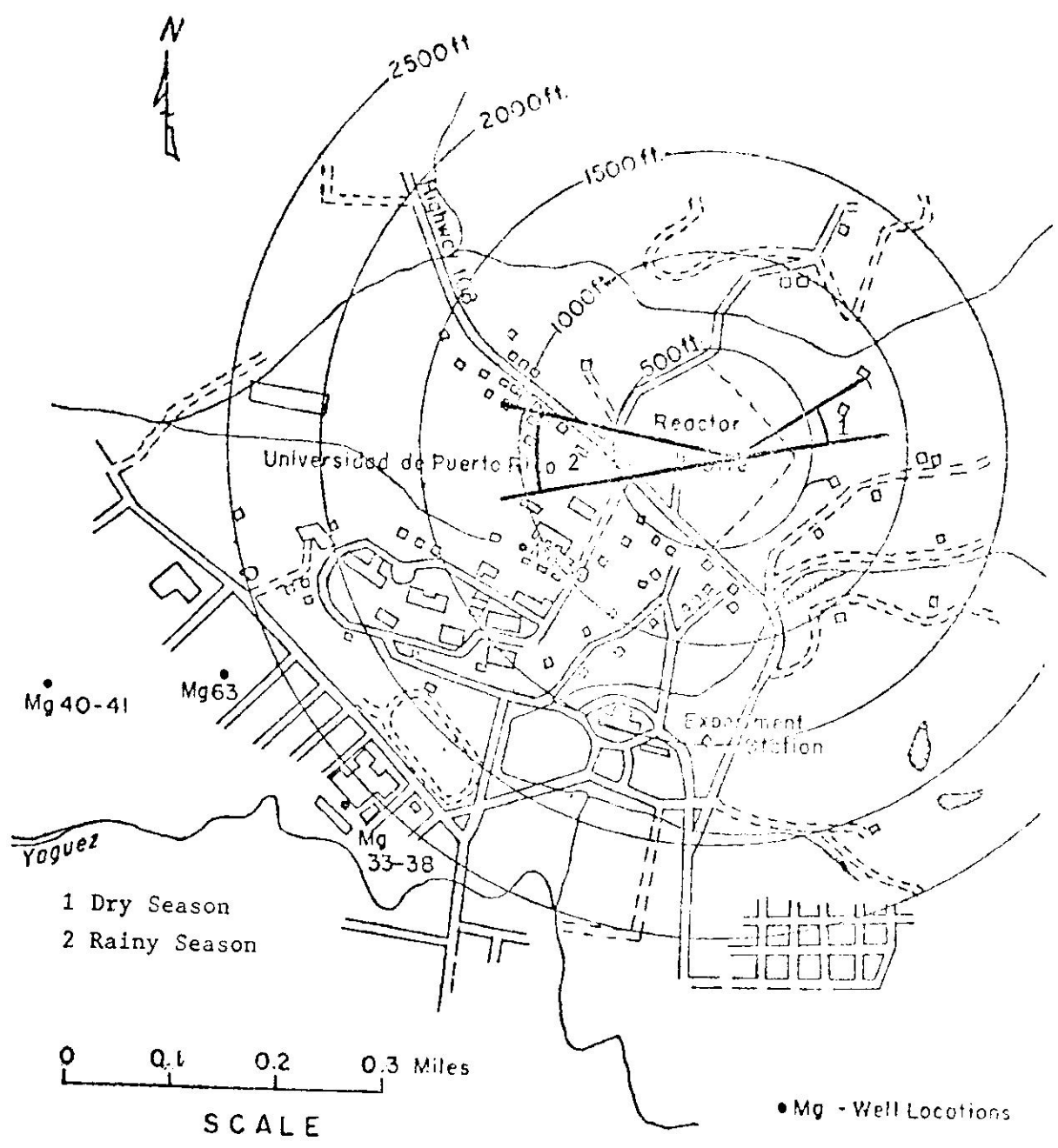


Figure 9. Map of the Reactor Site Showing the Location of the Yearly Average Maximum Concentration.

T_R = radioactive half life (sec)

T_B = biological half life (sec)

t = time of exposure (sec)

t' = time following exposure (sec)

D_{CO} = dose to the organ from internal radiation (rad)

When inhaled, argon is assumed to be distributed evenly through the lungs. The lungs are, therefore, the critical organs and $M = 1000$ gm using the standard man. (10).

The energy absorbed from the beta and gamma radiation of argon-41 was assumed to be one third of the end-point energy of the beta and to be the amount of gamma energy absorbed when passing through 10 cm of lung matter, as is given in Equation 7.89 of (9).

$$E = \frac{E_\beta}{3} + E_\gamma(1 - e^{-\mu r})$$

μ = the energy absorption coefficient of the lung for the gamma photon (cm⁻¹)

r = the effective diameter of the organ (cm)

E_λ = gamma energy per desintegration (Mev)

E_β = end point energy of the beta (Mev)

The fraction of the radionuclide, transferred to the organ by inhalation, f_a , is assumed to be 0.10, as recommended by Dr. Theodore Agard. (11).

The breathing rate, B' , for standard man was assumed to be 2.78×10^{-4} meters³/sec.

The biological half-life for argon-41 is short, but not well known. A value of 30 sec was assumed, knowing that xenon, also a noble gas, has a biological half-life of less than 30 sec (11). Therefore, the effective decay constant, λ , is 0.0232 sec⁻¹.

Table 7. Yearly Average Maximum Concentration and Dose Calculations

Sector of Maximum Concentration	Distance from the Source X (Meters)	Wind Frequency f (%)	Wind Speed u (Meters/sec)	Meteorological Conditions	Height of Source h (Meters)	Emission Rate Q' (Ci/sec)	Yearly Average Maximum Concentration X (Ci/Meter) ³	Internal Dose Average Day D _{co} (mrem)	Yearly Average Maximum Dose (mrem)			
									Average Day	Average Week (5 days)	Average Year (35 Week Rainy, 17 Week Dry)	
One-Shift 7:30 A.M.- 3:30 P.M.												
Dry Season	ENE 125	12.1	3.26	Adiabatic	10	9.0X10 ⁻⁶	2.69X10 ⁻¹⁰	2.80X10 ⁻⁶	4.6X10 ⁻³	2.32X10 ⁻²		
Rainy Season	W 275	8.1	3.00	Adiabatic	20	9.0X10 ⁻⁶	4.43X10 ⁻¹¹	4.62X10 ⁻⁷	7.6X10 ⁻⁴	3.82X10 ⁻³		0.53
Two-Shift 7:30 A.M.- 11:30 P.M.												
Dry Season	ENE 125	11.0	3.31	Adiabatic	10	9.0X10 ⁻⁶	2.41X10 ⁻¹⁰					
	ENE 125	0.6	0.09	Large Inversion	10	9.0X10 ⁻⁶	2.74X10 ⁻²¹	3.45X10 ⁻⁶	5.7X10 ⁻³	2.86X10 ⁻²		
Rainy Season	W 275	9.4	3.04	Adiabatic	20	9.0X10 ⁻⁶	5.08X10 ⁻¹¹					0.70
	W 275	24.4	2.95	Large Inversion	20	9.0X10 ⁻⁶	1.33X10 ⁻²⁴	7.28X10 ⁻⁷	1.2X10 ⁻³	6.00X10 ⁻³		

The exposure time, t , equals eight hours for one shift operations and eleven hours for two-shift operations. The concentration of argon-41 during the last five hours of two-shift operation is more than ten orders of magnitude less than the concentration for the day-time operation and is therefore neglected. The dose received after exposure has stopped ($t = 300$ sec). This is ten times the assumed biological half life.

The results of the internal dose calculations for an average day in mrem are given in Table

To convert from rad to rem a relative biological effectiveness (RBE) factor is needed which for gammas and betas is equal to one.

2. External dose calculations

The external dose in a homogeneous infinite cloud was calculated by adding the contribution due to the beta and gamma radiation. The calculation was made using Equations 7.20 and 7.35a from Reference 9.

$$D' = (0.23 E_{\beta} + 0.25 E_{\lambda}) \bar{X}$$

where

\bar{E}_{β} = end point energy of the beta (Mev)

\bar{E}_{λ} = gamma energy per desintegration (Mev)

\bar{X} = yearly average maximum concentration (Ci/meters³)

D' = dose rate (rad/sec)

In calculating the yearly average maximum dose, internal plus external, the internal dose can be neglected since it is a factor of a thousand less than the external dose. (See Table 7).

DISCUSSION OF RESULTS

A. OVERALL EFFICIENCY DETERMINATION OF THE DETECTION SYSTEM FOR THE 1.29 Mev GAMMA OF ARGON-41

The Scintillation Spectrometry Gamma-Ray Spectrum Catalogue (Appendix II), (7) indicates that the total spectral efficiency of a standard four inch diameter by four inch deep sodium iodide detector in response to a sodium-22 point source, 7.88 cm above the detector should be 4.2%. In addition, this same reference gives the peak to total spectrum ratio for sodium-22 in a three inch diameter by three inch deep detector as 0.35. This implies that we might expect our system to have an efficiency of $4.2\% \times 0.35 = 1.5\%$ rather than 1.31%. This difference is possibly explained by : a) different techniques used in obtaining the peak spectra (The Spectrum Catalogue does not discuss the technique used in obtaining the peak spectrum), b) a lower intrinsic efficiency of our detector due to detector fatigue or other reasons (our detector is eight years old) and c) lower efficiency of the electronic components of our system.

However, it should be noted that the accuracy of the measurement is not dependent upon determining the absolute efficiency of the system, but rather upon using a technique which assures that the ratio of counts of the detector to activity of a source is the same for argon-41, cesium-137, and sodium-22.

Thus the ratio

$$\frac{\text{Counts under peak for Na-22}}{\text{Known activity of Na-22}} = 1.31\%$$

Using Figure 2 to extrapolate from the 1.27 Mev gamma peak of the sodium-22 to the 1.29 Mev gamma peak of argon-41 we obtain

$$\frac{\text{Counts under peak for A-41}}{\text{Known activity of A-41}} = 1.30\%$$

and this is the value we have used for the efficiency of the system.

It should be noted that great care was taken in determining the efficiency of the system, since all succeeding work depends upon the efficiency and since our value of 1.29% differs by 30% from the value of 1.8% obtained by Efigenio Rivera (2).

B. DETERMINATION OF THE ARGON-41 CONCENTRATION

1. In the off gas system

The average argon-41 concentration and emission rate for 1000 Kw power level were found to be $10.80 \times 10^{-5} \pm 0.37 \times 10^{-5}$ $\mu\text{Ci/cc}$ and 543 ± 17.5 $\mu\text{Ci/min}$, respectively. The difference between these values and the ones used by Efigenio Rivera (2), 2.7×10^{-5} $\mu\text{Ci/cc}$ and 116.1 $\mu\text{Ci/min}$ are due to the difference in the efficiency and flow rate measurements.

a. Kanne chamber calibration

An estimation of the accuracy of the Kanne chamber reading can be obtained from Table 1 and Figure 3. At a constant indicated power level of 1000 Kw, both the Kanne chamber reading and the concentration as determined in the experiment show a variation of approximately 5% around the mean value. However, it is not known which part of the variation should be attributed to errors in the indicated power level, the concentra-

tion and the Kanne chamber reading. In addition, the Kanne chamber can be read to only two significant figures, this in itself gives a possible error of approximately 2%.

The conversion factor of $2.3 \times 10^{+6} \pm 0.06 \times 10^{+6}$ $\mu\text{Ci}/\text{cc}$ per amp found contains seven of the nine data points, as indicated in Figure 3. It is therefore concluded that the best estimate in error in converting Kanne chamber reading to concentration is approximately 5%.

B. Emission rate variation with power level

The linearity of the emission rate of argon-41 production as a function of power level was determined with a 6% probable error.

2. At the surface of the reactor pool

The argon-41 concentration and the emission rate measured at the surface of the reactor pool are 6.383×10^{-3} $\mu\text{Ci}/\text{cc}$ and 1.7 $\mu\text{Ci}/\text{min}$ respectively

3. At various ground level locations

a. Sensitivity of counting system

As discussed in Section III-B-3, three modifications were made to the standard system in order to improve the sensitivity of the system for counting argon-41. They were: a) increasing the shielding to six inches of lead, b) connecting two sodium iodide detectors in parallel, and c) collecting air in a scuba tank at a pressure of 2200 psi.

An indication of the accuracy of the system, with both detectors and

increased shielding was obtained by determining the half life of argon-41 using the decay constant obtained as $1.042 \times 10^{-4} \text{ sec}^{-1}$.

$$T_{1/2} = \frac{\ln 2}{\text{Decay Constant}} = 1.85 \text{ hours}$$

The half life of argon-41 reported by Lederman (12) is 1.83 hours, however, he refers to three works which report 1.83 hours, one which reports 1.82 and the other which reports 1.85 hours. The initial to final count ratio of approximately 4500 indicates the sensitivity of the counting system considering only the first two modifications. However, the sensitivity was increased by a factor of 150 by collecting air in a scuba tank at a pressure of 2200 psi. Therefore, when the three modifications were combined, the argon-41 concentration at ground level could be read to approximately $1.6 \times 10^{-10} \mu\text{Ci/cc.}$, which is less than 20% of the allowed concentration of $8.0 \times 10^{-10} \mu\text{Ci/cc}$ with a probable error of not more than 10%.

b. and c. Measured and calculated values

The average value of the ratio of the estimated to measured concentration is 1.1. The low frequency case (run No. 2 of Tables 4 and 6) was not included in this average because the equation we used for estimating the concentration is for long term average release. An implicit assumption in this equation is that the percent of time the gas leaves the stack, in the direction of a given sector, is equal to the percent of time the gas is found in the sector at some distance X from the stack. This will be true for both low and high frequency in

a sector during a long period of time such as a year since the cross wind component is insignificant for the high frequency situation, and since for the low frequency case the cross wind components in a sector would be self compensating. However, for a short period of time, such as the half hour period, during which our samples were collected, this equation will only be applicable for the high frequency situations. For the low frequency case and short collection time the model does not apply due to the fact that when the crosswind component is in a constant direction, very little, if any, of the gas entering a sector of the stack would still be in that sector a significant distance from the stack.

The excellent agreement between the measured and estimated concentrations serves as a verification of the model used and gives a high degree of confidence that the calculated yearly average maximum concentrations are accurate.

d. Yearly average maximum concentration

The previous value used for the yearly average maximum concentration, one-shift, dry season was 1.63×10^{-10} Ci/meters³ (13), where the value obtained in this study is 2.69×10^{-10} Ci/meters³. Since the presently allowable value is 8.0×10^{-10} Ci/meters³, which is 2% of the allowable value specified in 10 CFRM Part 20, Appendix B, Table II, Column I, (1) the yearly average maximum concentration is 33.6% of the allowable.

C. YEARLY AVERAGE MAXIMUM DOSE CALCULATIONS

The previous value used for the yearly average maximum dose one-shift, dry season was 0.45 mrem (13), where the value obtained in this study is

0.53 mrem. Since the presently allowable value is 10 mrem, the yearly average maximum dose is 5.3% of the allowable.

It can be noted that if a person is exposed to the daily average maximum dose, not for one-shift operation but rather for 24 hours a day, seven days a week, then the dose would be 50% of the allowable. These values seem to indicate a reasonable correlation between the concentration and dose.

CONCLUSION

The Kanne chamber appears to be satisfactorily calibrated with a probable error of approximately 5%.

The emission rate was found to be linear as a function of power. The average emission rate for 1000 Kw, with all of the off-gas facilities connected, was determined to be 543 $\mu\text{Ci}/\text{min}$, with a probable error of 6%.

The system using improved shielding, parallel detectors, and scuba tank allows concentration at ground level to be measured to a factor of 6.75×10^5 less than the concentration emitted by the off-gas stack, or to approximately 1.6×10^{-10} $\mu\text{Ci}/\text{cc}$.

The average value of the ratio of the estimated to measured concentration is 1.1. This excellent agreement between the measured and estimated concentrations gives a high degree of confidence in utilizing the diffusion equation for average long-period concentration from a continuous point source to calculate the yearly average maximum concentration.

The largest value of the yearly average maximum concentration occurred during one-shift operation, dry season, at 125 meters from the stack in the ENE sector. This value was found to be 2.69×10^{-10} $\text{Ci}/\text{meters}^3$, which is 33.6% of the allowable value as proposed in June, 1974. (1)

The dose corresponding to the largest yearly average maximum concentration is 0.53 mrem per year, which is 5.3% of the allowable value.

Since the concentration and dose are 33.6% and 5.3% of the allowable values, respectively, argon-41 emission is not a limiting value for the

PRNC TRIGA-FLIP reactor operating at 1000 Kw. Although for 2000 Kw operation, the concentration and dose would double, the concentration would still be approximately 70% of the allowable and probably indicates a safe operating condition.

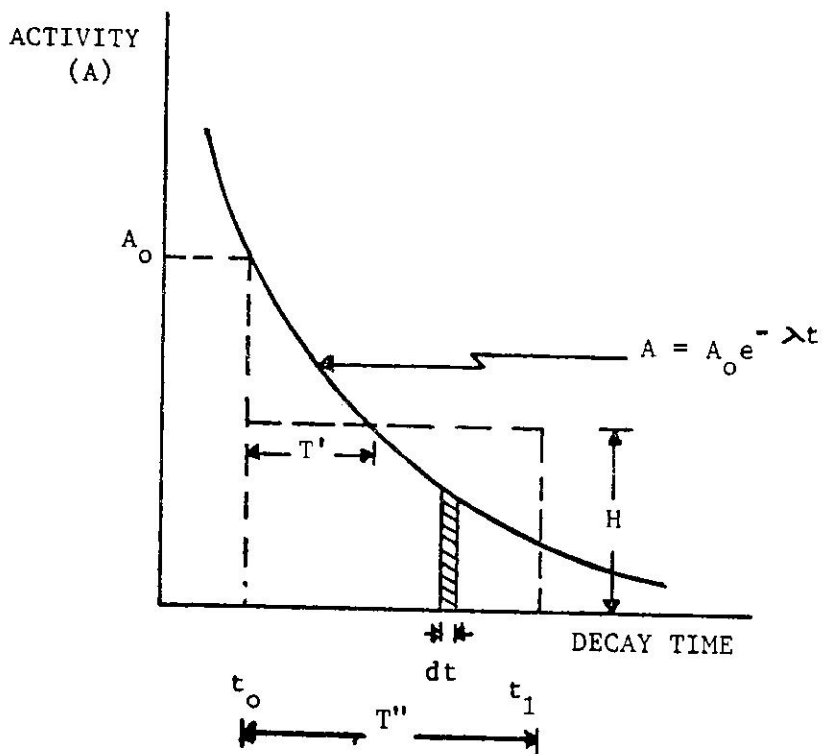
REFERENCES

1. "Draft Standard for Restrictions on Radioactive Effluents from Research Reactors", Private Communication between Joseph A. Lenhard, Director, Research and Technical Support Division, Oak Ridge National Laboratories to Dr. Lawrence S. Ritchie, Director, Puerto Rico Nuclear Center, June 23, 1974.
2. Rivera, E., "A Method to Determine Gaseous Effluents from the Puerto Rico Nuclear Center TRIGA-FLIP Reactor, Mayaguez, Puerto Rico", Master of Science Thesis, Univ. of Puerto Rico, RUM, April 1973.
3. Cruz, P., "Kanne Chamber Calibration", Puerto Rico Nuclear Center Internal Document, Puerto Rico Nuclear Center, Mayaguez, Puerto Rico, (1968).
4. Fitzgerald, J.J. and Borelli, B.W., "Determination of Efficiency of Kanne Chamber for Detection of Radiogases," Report No. KAPL-1231 Health and Biology (TID-4500) 8th ed., (1954).
5. Kanne, W.R., "Monitoring of Gas for Radioactivity," United States Patent Office, Patent No. 2599922, Patented June 10, 1952, Filed October 12, 1944.
6. Kanne, W.R., "Monitoring Gas for Radioactive Xenon," United States Patent Office, Patent No. 2625657, Patented January 13, 1953, Filed November 28, 1945.
7. Health, R.L., Scintillation Spectrometry Gamma-Ray Spectrum Catalogue, TID-4500 (31st ed.), August, 1964.
8. "Hazard Summary Report for the Pool-Type Research Reactor at the Puerto Rico Nuclear Center in Mayaguez, Puerto Rico", PRNC-37, December, 1964.
9. Slade, D.H., Editor, Meteorology and Atomic Energy 1968, TID-24190, Clearinghouse for Federal Scientific and Technical Information, National Bureau of Standards, United States Department of Commerce, Springfield, Virginia 22151, July, 1968.
10. Wang, Yen, M.D., Editor, Handbook of Radioactive Nuclides, The Chemical Rubber Co., (1969).
11. Agard, E.T., Division Head of Medical Physics, Puerto Rico Nuclear Center, Private Communications, March, 1975.
12. Lederer, C.M., Hollander, J.M., Perlman, I., Table of Isotopes, 6th ed., John Wiley and Sons, Inc., (1967).

13. Brown, R., Sasscer, D., Rivera, J.E., "Measurement of Argon Releases at the Puerto Rico Nuclear Center Triga Reactor and Calculations of the Radioactive Argon Concentrations and Dose", Internal Puerto Rico Nuclear Center Document, June 1974.

APPENDIX

DECAY TIME



where

A_0 = activity at start counting time

$T'' = (t_1 - t_0)$ = counting time period

H = average activity for the counting time period

T' = time from start counting until average activity is reached

Therefore, it can be stated that

$$\text{Area} = HT'' = \int_{t_0}^{t_1} A dt$$

$$= A_0 \int_{t_0}^{t_1} e^{-\lambda t} dt$$

$$= \frac{-A_0}{\lambda} (e^{-\lambda t}) \Big|_{t_0}^{t_1}$$

let $t_0 = 0$

$$t_1 = T''$$

then

$$HT'' = \frac{A_0}{\lambda} (e^{-\lambda T''} - 1)$$

or

$$H = \frac{A_0}{\lambda T''} (1 - e^{-\lambda T''})$$

but

$$H = A_0 e^{-\lambda T'}$$

therefore

$$T' = \frac{1}{\lambda} \ln \left(\frac{\lambda T''}{1 - e^{-\lambda T''}} \right)$$

now for

$$T'' = 10000 \text{ seg}$$

and

$$\lambda_{\text{ar-41}} = \frac{\ln 2}{1.83 \text{ hr.}} \left(\frac{\text{hour}}{3600 \text{ sec}} \right) = \frac{1.052(10^{-4})}{\text{sec}}$$

we have the following

$$T' = \frac{1}{1.052(10^{-4})} \ln \left(\frac{(1.052)(10^{-4})(10000)}{(1 - e^{-1.052(10^{-4})(10000)})} \right)$$

or

$$T' = 4566 \text{ sec}$$

The following is a table containing all the T' corresponding to the counting periods used.

$T''(\text{seg})$	$T'(\text{seg})$
100	49.96
4K	1930
10K	4566
20K	8307

The fact that time had passed from the sample collection time to the start counting time was taken into consideration. So the total decay time is

$$T = T + T'$$

where

T' = decay correction time during counting

T = time between collection and start counting

In the case where the tank was filled up to a pressure of 2200 psi, the pumping time must also be considered. The pumping time was measured and it was determined that the rate of air entering the tank is a constant function with time, therefore, T to determine decay time is equal to half of the pumping, plus the time between the end of pumping and the start of counting.

“This paper was prepared in connection with work under Contract No. E-(40-1)-1833 with the U.S. Energy Research Development Administration. ERDA retains a non-exclusive royalty-free license in and to any copyrights covering this paper, with the right to authorize others to reproduce all or any part of the copyrighted paper”